



Low and high-pressure hydriding of V–0.5at.%C

Joshua Lamb^a, Dhanesh Chandra^{a,*}, Michael Coleman^a, Archana Sharma^a, William N. Cathey^a, Stephen N. Paglieri^b, Joseph R. Wermer^c, Robert C. Bowman Jr.^d, Franklin E. Lynch^e

^a University of Nevada, Reno, M.S. 388, Reno, NV 89557, USA

^b TDA Research, Inc., 12345 W. 52nd Ave., Wheat Ridge, CO 80033, USA

^c Los Alamos National Laboratory, P.O. Box 1663, MS-C927, Los Alamos, NM 87545, USA

^d Jet Propulsion Laboratory, California Institute of Technology, Mail Stop 79-24, Pasadena, CA 91109, USA

^e HCL, 12400 Dumont Way, Littleton, CO 80125, USA

ARTICLE INFO

Article history:

Received 25 March 2009

Accepted 4 January 2010

ABSTRACT

The low-pressure hydriding characteristics of V–0.5at.%C alloy were determined in this study. There are several prior reports on the pressure-composition-temperature (p–c–T) isotherms and stability of the low-pressure vanadium hydride phases (V_2H or β_1), and of vanadium alloyed with transition elements, but there are no reports on the hydrides of V–C alloys. The thermodynamic properties of the vanadium did not change significantly with the addition of carbon. In addition to low-pressure studies on V–0.5at.%C, we also performed high-pressure studies on $V_2H \leftrightarrow VH \leftrightarrow VH_2$ ($\beta_1 \leftrightarrow \beta_2 \leftrightarrow \gamma$) hydrides, including thermal cycling (778 cycles) between the β and γ phases. Thermal cycling between $VH \leftrightarrow VH_2$ increased the pressure hysteresis. The effects of thermal cycling (4000 cycles) on the absorption and desorption isotherms of V–0.5at.%C and on the H/M ratios for the β_1 -, β_2 - and γ -phase hydrides are also presented. There was minimal decrepitation (pulverization) of the alloy; decrepitation of the V–0.5at.%C alloy was dramatically less than that of pure vanadium.

© 2010 Elsevier B.V. All rights reserved.

1. Introduction

Metal hydrides and metal hydrogen interactions form the basis for several important technologies used in nuclear fusion power plants; applications include the storage, separation, and purification of hydrogen isotopes (protium, deuterium, and tritium). For example, hydrogen permeable metal alloys have recently gained importance as membranes for hydrogen purification. Metal membranes are used to aid the recovery of gaseous hydrogen isotopes from fusion reactor exhaust [1–8]. The use of membranes has also been proposed to control the hydrogen isotope concentration in fusion reactors and to extract tritium from molten metal breeder reactor blankets [9–15]. Typically, Pd–Ag alloys such as Pd₇₇Ag₂₃ are used for these separations.

Although palladium alloys are already being used, the high cost of palladium has driven the search for alternative and relatively cheaper materials, such as vanadium alloys, as potential membrane materials [16–19]. Whether the membrane maintains its integrity after several heating and cooling cycles under differential gas pressure depends on the types of hydrogen solid solutions and reversible low-pressure hydrides that are formed. Since membranes are used to purify hydrogen from a mixture of gases under differential pressure, it is important to understand the gas phase

(as opposed to electrochemical) charging of vanadium to form hydride phases. Operating in the solid solution region is important to ensure that there are no abrupt volume expansions due to hydride phase formation. Therefore, it is of value to suppress the formation of brittle hydride phases. Vanadium alloys do a better job maintaining their integrity during thermal cycling in hydrogen than does the pure metal [19–23]. Vanadium alloys have also been shown to have higher hydrogen permeabilities than palladium alloys [19].

Both palladium and vanadium have also been used to separate hydrogen isotopes due to the strong isotope effects in some of their hydride phases [24–27]. Hydrogen isotopes are separated from each other in a semi-batch chromatographic column using either pressure or temperature swing absorption [27]. For example, in the thermal cyclic absorption process (TCAP), palladium supported on kieselguhr (diatomaceous earth) is used to separate binary mixtures of hydrogen isotopes. Although vanadium has been studied as an absorbent, it is important that the chromatography column packing material resists decrepitation (pulverization) as it is subjected to repeated hydriding/dehydriding cycles. However, pure vanadium is known to break down into micron-sized particles in the presence of hydrogen [28].

Vanadium has also been explored as a hydrogen storage material because of its high volumetric density [29]; it is a good candidate material for hydrogen isotope storage and stationary hydrogen energy applications where weight is only a secondary

* Corresponding author. Tel.: +1 775 784 4960; fax: +1 775 784 4316.
E-mail address: dchandra@unr.edu (D. Chandra).

consideration. However, the reversible hydrogen capacity of vanadium is rather low (i.e., ~2 wt.%) compared to the lithium and magnesium materials presently under development for vehicular hydrogen storage [30].

Fagerstroem et al. provided a compilation of various reports on thermodynamic and crystallographic investigations of the stable phase regions in the V–H binary system, specifically regarding the formation of the three hydride phases, V₂H (β_1), VH₁ (β_2), and VH₂ (γ) [31]. Reilly and Wiswall reported two plateaux in the isotherm. The following equations describe the formation of β_1 phase from the α -phase solid solution [32]:



the formation of β_2 phase from β_1 ;



and the formation of γ phase from β_2 phase;



Experimental results and pressure-composition-temperature (p–c–T) isotherms at low-pressures were reported by Fujita et al., Griffiths et al., and Schober for pure vanadium [33–35]. The V₂H (β_1) and VH (β_2) phases were very stable and do not exhibit hydrogen desorption at moderate conditions [33]. For example, the plateau pressure for V₂H formation was 0.1 Pa, thus indicating a very stable phase. However, the fully hydrogenated γ phase was much less stable than the β phases and, thus, the hydride phase transition (reversal of $\beta_2 \leftrightarrow \gamma$) could be observed at relatively low temperatures [32,36].

Past researchers focused on stabilizing the γ phase through the addition of alloying elements [37–42]. Recent investigations by Yukawa et al. have focused on stabilizing both the β and γ phases by the addition of alloying elements (V–1 mol%M and V–3 mol%M where M is a 3d-, 4d-, or 5d-transition metal) [43,44]. Furthermore, low-pressure isotherms of V–3%M obtained at 343 K exhibited increasing $\alpha \leftrightarrow \beta_1$ plateau pressures when $M = \text{Ti, Cr, Mn, Fe, Co, and Ni}$. They demonstrated increased stability of the γ phase with the addition of alloying elements (stability varied with the position of the element in the periodic table), however, they were unable to conclusively address the reversal of $\beta_1 \leftrightarrow \alpha$ phase [44]. In a subsequent study, they addressed the stability of the β phases as a function of transition group alloying elements at low-pressure, and other work by this group involved a novel electrochemical apparatus for determining the p–c–T curves. To understand the effect of alloying elements on the β phases, these systematic studies by Yukawa et al. were the first to be reported in the literature.

Concurrent to our research on the metal hydrides of several AB₅ alloys [45–48], the effects of thermal cycling on the hydriding performance of VH_x hydrides have been reported [28]. We present a combination of earlier results, corroborated with recent experiments, on the effect of carbon as an alloying element on the hydriding properties of vanadium [49,50]. According to the V–H phase diagram, it is possible to observe the vanadium–hydrogen solid solution (α phase) at temperatures above 473 K [31]; isotherms are measured at higher temperatures (>473 K) for V–0.5at.%C hydrides. A particular concern that we investigated is the inherent problem of microstrain development during γ phase formation during high-pressure hydriding, leading to large desorption pressure hysteresis after thermal cycling.

Therefore, experiments were performed over a broad range of temperatures and pressures to understand the behavior of V–C–H phases for possible use in hydrogen isotope separation, purification and storage technologies. High-pressure experiments were undertaken to understand the effect of thermal cycling on absorption and desorption plateau pressures. These studies led to some

interesting results on the apparent increased resistance of V–0.5at.%C to hydrogen induced decrepitation. An advantage of alloying vanadium with carbon is that it has the potential to minimize the plastic deformation or premature fracture of containers for vanadium hydrides due to large volume changes during the $\beta_2 \leftrightarrow \gamma$ phase transformation [38]. First, we reported low-pressure gas phase charging to obtain $\alpha \leftrightarrow \beta_1$ isotherms for V–0.5at.%C at several temperatures, and then high-pressure isotherms ($\beta_2 \leftrightarrow \gamma$) at 298 K. X-ray and scanning electron microscopic characterization of the materials were also shown. Some data has been presented in this paper on thermal cycling between the $\beta_2 \leftrightarrow \gamma$ phases, although more details may be found in Sharma et al. [49,50].

2. Experimental

High purity (99.99%) vanadium crystals (lot #11) obtained from the US Bureau of Mines were used as reference samples. The V_{0.995}C_{0.005} (V–0.5at.%C) samples were made by alloying vanadium metal with VC (98.8% purity) obtained from Alpha Aesar. Ultra high purity (99.9995%) hydrogen, helium, and argon were used for the experiments. Alloys were made by arc-melting the two components, forming buttons that were re-melted five different times. These buttons were wrapped in Ta foil, and annealed at 1473 K for 24 h in evacuated stainless steel containers. The buttons were quickly cooled to room temperature (to avoid the formation of V₂C precipitates) and cut into pieces for use in various experiments.

An automated Sieverts' apparatus was used for obtaining low-pressure p–c–T isotherms for V–0.5at.%C. A small palladium wire was used for activation purposes and did not affect the results [44]. An MKS Baratron pressure transducer (Model No. 690A01TRB) was used for pressure measurements up to ~133 Pa. High-pressure experiments were performed in a Sieverts' apparatus in collaboration with Frank Lynch at HCL, Littleton, Colorado [51]. In this case, the system was calibrated using a dead weight tester and mercury manometer. For the high-pressure experiments, the sample holder was placed in a water bath maintained at 298 K. The compressibility of hydrogen gas was taken into account by using virial coefficients. Thermal cycling experiments were performed by using four separate sample holders described in more detail by Lambert et al. [45]. The experiments were conducted over a temperature range of 323–523 K as the low-pressure hydride phases do not typically form over 523 K [52].

3. Results and discussion

Pressure-composition isotherms of V–0.5at.%C taken at several temperatures are presented in Fig. 1 to show the variation in $\alpha \leftrightarrow \beta_1$ plateau pressures compared to pure vanadium. Increases in plateau pressure can be observed for isotherms taken between 323 and 535 K. The $\alpha \leftrightarrow \beta_1$ phase boundaries compiled in Table 1 are extracted from the data in Fig. 1; as shown, the formation of β_1 hydride phase is limited to temperatures less than ~450 K. Comparison of the phase boundaries of the V–H binary system to the values listed in Table 1 suggests solid solution α phase formation at 473, 498, and 523 K. The absence of hydride formation in the V–0.5at.%C–H system above approximately 450 K is of importance to membrane technologies that must operate without distortion and embrittlement.

The equation for the $\alpha \leftrightarrow \beta_1$ plateau pressure was developed from isotherms taken between 398 and 448 K. The van't Hoff plots derived from this data are shown in Fig. 2. The data point taken at 323 K was not included in the enthalpy calculation because the isotherm plateau pressure deviated substantially from other work that showed much lower isotherm pressures at this temperature

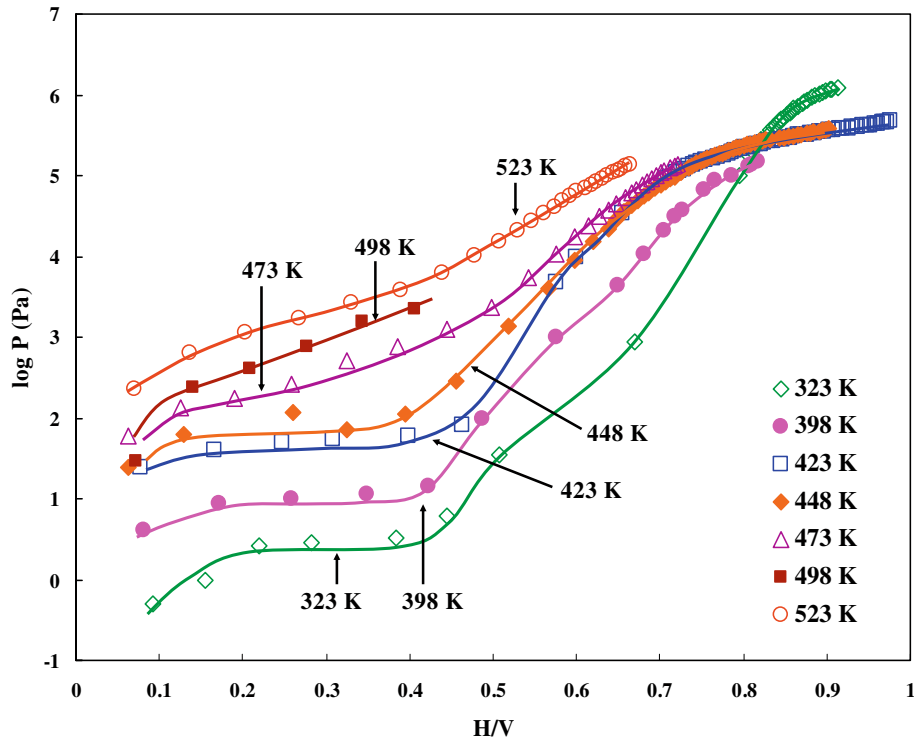


Fig. 1. Pressure-composition isotherms for V-0.5%C taken at several temperatures showing the $\alpha \leftrightarrow \beta_1$ plateaux.

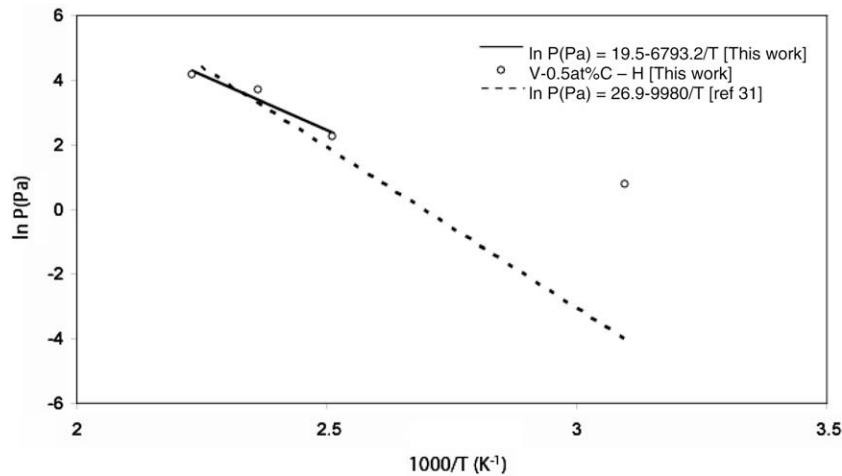


Fig. 2. A van't Hoff plot for V-0.5at%C showing the temperature dependence of plateau pressure. Data from Fagerstroem et al. included for comparison [31].

for pure vanadium [43]. The equilibrium hydrogen pressure equations for vanadium and V-0.5at.%C hydrides are given in Table 1.

The phase boundaries from the V-H phase diagram were used to identify the formation of β_1 hydride based on the plateaux observed in the isotherm. Corresponding phase stabilities at various temperatures from the isotherm data of this study compare well with the boundaries in the established V-H phase diagram [31]. It can be noted that as the pressure changes as a function of hydrogen content, the low-pressure isotherms exhibit a rather complex shape. For example, the higher H/M portion of the curve for the isotherm at 323 K shows a different shape as compared to isotherms measured between 373 and 448 K; this corresponds well with the V-H phase diagram. At temperatures above ~ 450 K, the $\alpha \leftrightarrow \beta_1$ plateau does not exist, suggesting the presence of solid solution α phase as the hydrogen content increases. This may have signifi-

Table 1
Equations describing the hydrogen equilibrium pressure for vanadium and V-0.5at.%C.

Material	Equation (Pa)	Temperatures (K)	ΔH (kJ/mol)	ΔS (kJ/mol)
V-0.5%C-H	$\ln P = 19.5 - 6793.2/T$	398–423	-60	-66
V-H [43]	$\ln P = 26.9 - 9980/T$	365–463	-83	-118.6

cance in the operation of hydrogen permeating membranes, as formation of hydrides is detrimental to the long-term stability of membranes used at elevated temperatures. The phase boundaries for the low-pressure regions, based on the H/M ratios from the isotherms obtained at various temperatures, are presented in Table 2.

Table 2

Phase boundaries of V–0.5%C–H system determined in this study (CS = complete solid solution region).

Temperature (K)	H/M phase boundaries, Fig. 1		
	Stable α and $\alpha-\beta_1$ phase region	Single α or β_1 phase region	Single $\alpha-\beta_2$ phase region
323	0.02–0.48 ($\alpha + \beta_1$)	0.48–0.7 (β_1)	0.7–1 (β_2)
398	0.13–0.48 ($\alpha + \beta_1$)	0.48–0.65 (β_1)	0.65–1 (β_2)
423	0.26–0.47 ($\alpha + \beta_1$)	0.47–0.64 (β_1)	0.64–1 (β_2)
448	0.35–0.48 ($\alpha + \beta_2$)	0.35–0.48 (β_1)	0.48–1 (β_2)
473	α phase (CS)	α phase (CS)	α phase (CS)
498	α phase (CS)	α phase (CS)	α phase (CS)
523	α phase (CS)	α phase (CS)	α phase (CS)

High-pressure $\beta_2 \leftrightarrow \gamma$ isotherms from this study for pure vanadium are shown in Fig. 3. The low-pressure data of Griffiths et al. [34] are also included in Fig. 3 to show the progressive trend of pure vanadium hydrogenation from low to high-pressures [34]. There were no data collected between 0.1 and 31.6 kPa, so a dotted line is drawn to suggest the continuity of the isotherm to the data in the high-pressure region. The formation of α phase, the existence of an $\alpha \leftrightarrow \beta_1$ plateau and single β_1 and β_2 phase regions are all consistent with the features reported by Griffiths et al. for pure vanadium hydrides [34]. The maximum H/M value for pure vanadium in the present study agrees with the data of Reilly and Wiswall (H/M ~ 2 at 313 K) [32]. The high-pressure data of Luo et al. does agree in terms of plateau pressures, but their maximum H/M of 1.62 is quite low, compared to a value here of H/M = 1.95 at 298 K [53]. The reason for this discrepancy was explained as partial activation of their sample. The maximum H/M was also low for highly strained V–0.5%C alloy [49].

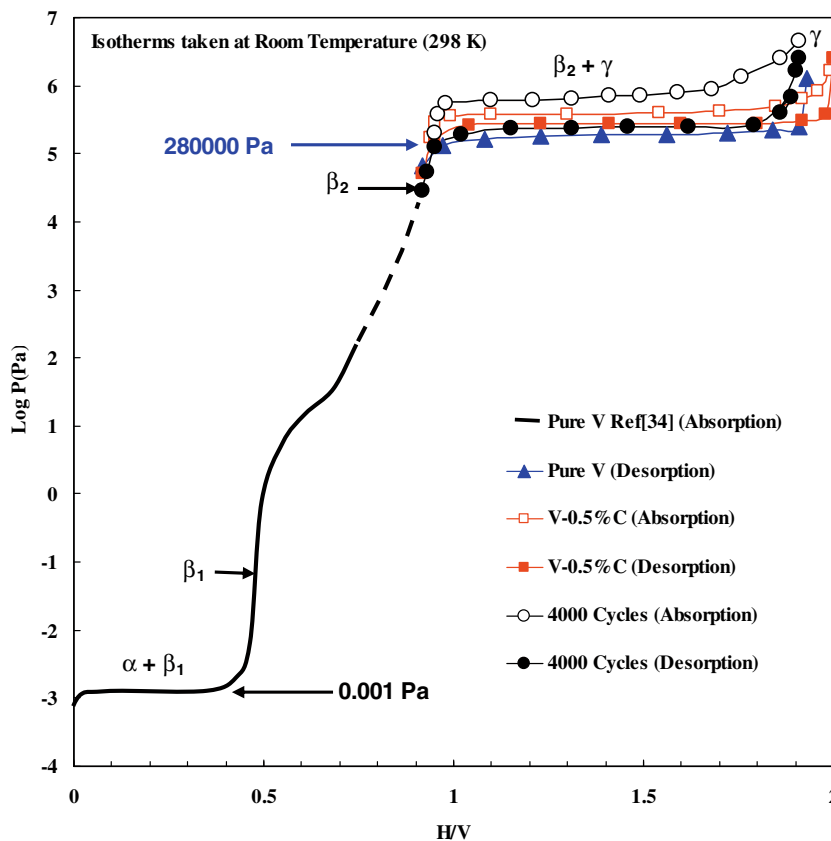


Fig. 3. Low- and high-pressure isotherms of pure vanadium from this work and Griffiths et al., and high-pressure isotherms of V–0.5at.%C at 298 K showing the α , $\alpha + \beta_1$, $\beta_1 + \beta_2$, and $\beta_2 + \gamma$ phase regions [34].

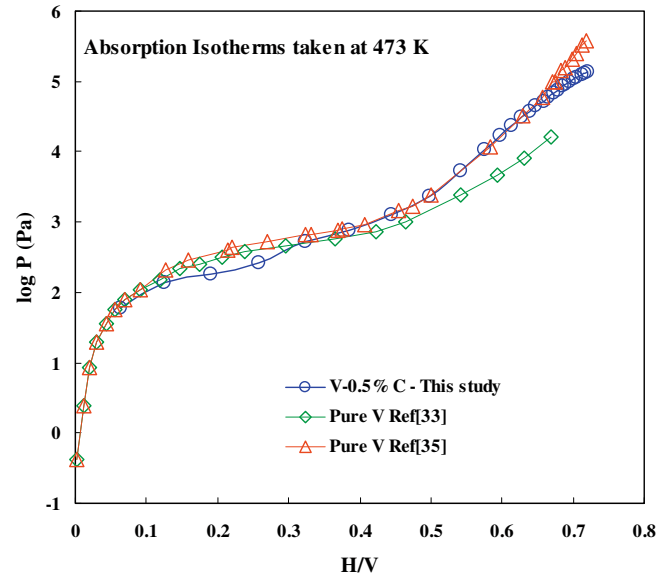


Fig. 4. Low pressure $\alpha \leftrightarrow \beta_1$ isotherm of V–0.5at.%C taken at 473 K. For comparison, data is also shown for pure vanadium taken at 473 K from Fujita et al. and Schober [33,35]. Note the agreement between the V–0.5at.%C and pure vanadium isotherms.

Fig. 3 displays the $\alpha \leftrightarrow \beta_1$ and $\beta_2 \leftrightarrow \gamma$ plateau continuity as a single plot. The high-pressure isotherms of V–0.5at.%C taken at 298 K show a $\beta_1 \leftrightarrow \gamma$ plateau at approximately 230 kPa (Fig. 3). From this isotherm, the hysteresis is comparable to that of pure vanadium after the first cycle (on an activated sample) [53]. There

is agreement between our pure vanadium hydride data, the low-pressure vanadium hydride data of Griffiths et al. taken at ~ 298 K, and the V–0.5%C isotherms shown in Fig. 3 [34]. Small changes in plateau pressure are attributed to the presence of carbon in the lattice.

The V–0.5at.%C hydride was subjected to prolonged thermal cycling (4000 cycles) between $\beta_1 \leftrightarrow \gamma$, after which the sample holder was attached to the Sieverts' apparatus to obtain isotherms (Fig. 3). It was apparent that desorption plateau pressures at all conditions were nearly the same, but the absorption pressure for the cycled

sample was relatively higher. Dislocation motion during hydriding may contribute to this affect since there was a large volume change during cycling between the $\beta_2 \leftrightarrow \gamma$ phases. Further details on these cycling experiments may be found elsewhere [49,50].

A comparison of isotherms obtained from this study with V–0.5%C, the pure vanadium data of Fagerstroem et al., and the data of Griffiths et al. show that the isotherms are virtually the same. This indicates that the solid solution effect of carbon on the thermodynamics of hydriding is minimal [31,34]. Apparently, higher concentrations of carbon are required to change the overall

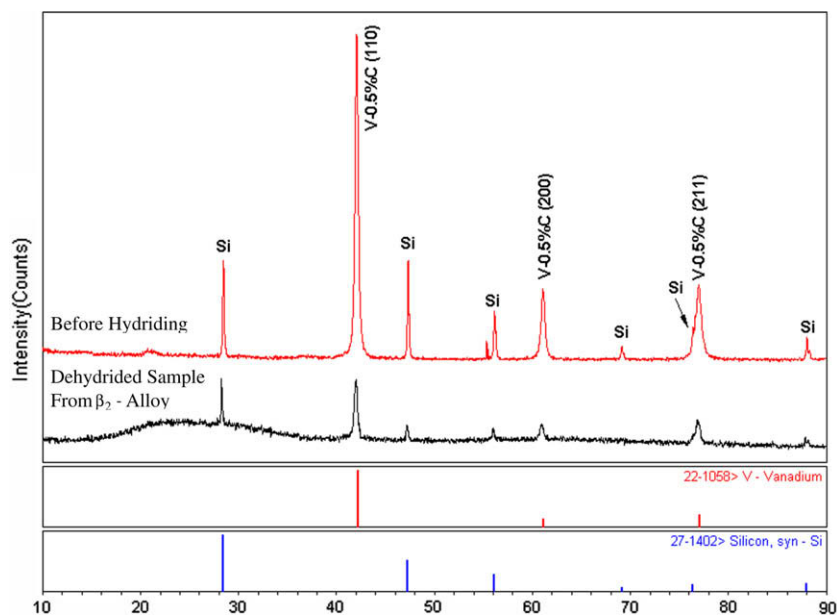


Fig. 5. X-ray diffraction patterns of V–0.5at.%C before and after low-pressure hydriding up to ~ 133 kPa. Analysis of the patterns show very little change in either the peak width or the Bragg angle, indicating complete reversal of the β_1 or β_2 hydride phases to V–0.5at.%C alloy. The high background in the pattern after hydriding is due to the substrate material used to mount the sample.

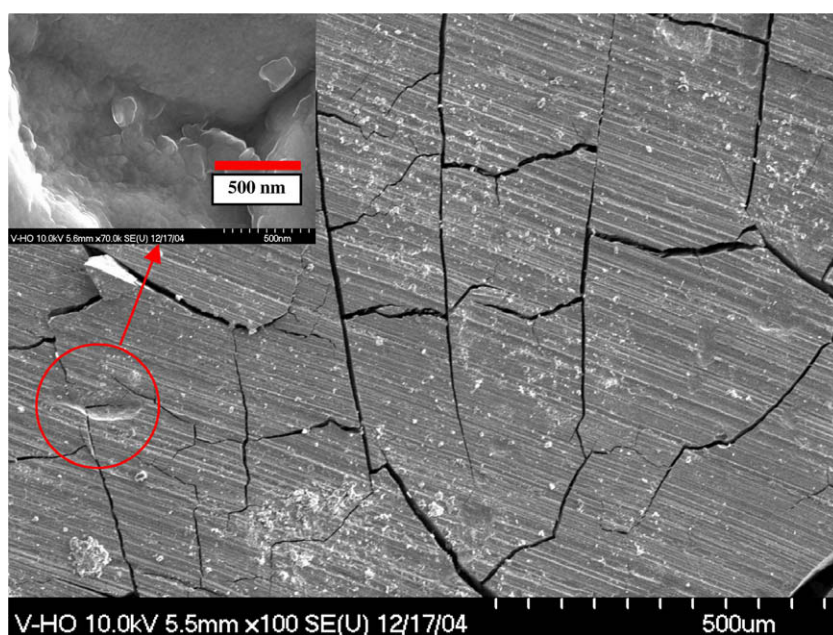


Fig. 6. SEM images showing fractures on the machined piece of V–0.5at.%C used for the hydriding experiments. The sample was thermally cycled continuously in hydrogen for the entire duration of experimentation (~ 8 months) with pressures up to ~ 133 kPa. The inset is a magnified image of the area in the circle showing details of the crack, indicative of very low porosity on the surface.

thermodynamics of the vanadium hydrogen system. Characterization of the low-pressure V–0.5%C sample by X-ray diffraction analyses before and after hydriding up to 1330 kPa showed very little change in either the peak width or the Bragg angle, indicating that there was essentially complete reversion of the β_1 or β_2 hydride phases to V–0.5%C alloy (Fig. 5). Furthermore, no trace of V_2C was observed in the XRD patterns, which suggests a vanadium–carbon solid solution.

Scanning electron microscopic (SEM) images (Fig. 6) showed that decrepitation of the alloy did not occur, except for some fissure formation on the surface. The sample was intermittently loaded with hydrogen and evacuated while conducting cycling experiments over a period of approximately eight months at pressures up to 1330 kPa. It should be noted that the original machining marks are still present after numerous pressure cycles, indicating very little degradation in structural integrity of the sample. In contrast, Bowman et al. [28] noted decrepitation, extensive formation of porosity, and a substantial increase in surface area for vanadium hydride samples subjected to one thousand thermal cycles across the $\beta \leftrightarrow \gamma$ mixed phase region. The results were an increase in the hydrogen absorption isotherm plateau pressures. The inset in Fig. 6 is a magnified image of the area in the circle revealing details of the fissure, representative of the low bulk porosity. Carbon apparently pins the dislocations since V–0.5at.%C is susceptible to plastic deformation, and a small amount of carbon may be effective in reducing the tendency for vanadium to experience brittle fracture and decrepitation.

Previous data by Luo et al. and Papanthanasopoulos and Wenzl [53,54] have shown that there is a negligible isotope effect on the low-pressure plateaux corresponding to the $\alpha + \beta$ two phase region, shown in Figs. 1 and 4. The higher-pressure plateaux (Fig. 3), shows lower pressures when exposed to deuterium [24]. The reaction with deuterium has also been shown to be more exothermic [53]. The V–C alloy studied here behaved similarly to pure vanadium in its hydrogen absorption, so it is expected to exhibit lower plateau pressures when exposed to hydrogen isotopes.

There also exists the possibility that the inclusion of carbon would have some effect on the permeation of hydrogen when used as a separation membrane. Notably, the low solubility of carbon in vanadium can lead to the formation of vanadium carbides (V_2C) at moderately high temperatures (≥ 1000 K) [55]. However, Hatano et al. [56] reported that the presence of V_2C did not significantly impede hydrogen permeation. Also, X-ray diffraction patterns collected in this study after exposure to hydrogen (Fig. 5) did not show evidence of carbide formation.

4. Conclusions

The low-pressure p–c–T isotherms of V–0.5at.%C alloy obtained by gas phase hydriding showed formation of V_2H (β_1) phase and compared well to literature data for pure vanadium. There was virtually no effect of carbon on the thermodynamics of hydride phase formation in vanadium. X-ray diffraction analyses showed that dehydrogenation from the β_1 to α phase was nearly complete to re-form the V–0.5at.%C alloy. There was minimal decrepitation of the alloy; decrepitation of the V–0.5at.%C alloy was dramatically less than that of either pure vanadium or the AB_5 series of alloys such as $LaNi_5$. Further studies should include the determination of optimum alloying and mechanical treatments to suppress hydride formation and increase the microstructural stability of the alloy during repeated thermal, pressure, and hydriding cycles.

Acknowledgments

We acknowledge Dr. Wen Ming Chien for assistance with plotting some of the figures, and Dr. Raja Chellappa, Dr. John D. Wright,

and Jan Graves for proofreading the manuscript. This work was funded in part by the US DOE and was partially performed at the Jet Propulsion Laboratory, which is operated by the California Institute of Technology under contract with the US National Aeronautics and Space Administration (NASA). The authors are also grateful for assistance by the DOE Metal Hydride Center of Excellence.

References

- [1] S. Charalambus, K. Goebel, Z. Naturforsch. A 20 (1965) 1085–1087.
- [2] H. Fujita, S. Okada, F. Fujita, H. Sakamoto, K. Higashi, T. Hyodo, J. Nucl. Sci. Technol. 17 (1980) 436–442.
- [3] V.V. Ishutin, B.N. Mekhedov, L.N. Sukhotin, J. Phys. Chem. 46 (1972) 1516–1517.
- [4] R.-D. Penzhorn, U. Berndt, E. Kirste, W. Hellriegel, W. Jung, R. Pejsa, O. Romer, Fusion Technol. 28 (1995) 723–731.
- [5] E.A. Clark, D.A. Dauchess, L.K. Heung, R.L. Rabun, T. Motyka, Fusion Technol. 28 (1995) 566–572.
- [6] B. Bornschein, K. Glugla, K. Gunther, R. Lasser, T.L. Le, K.H. Simon, Fusion Eng. Des. 69 (2003) 51–56.
- [7] S.A. Birdsell, R.S. Willms, Fusion Eng. Des. 39–40 (1998) 1041–1048.
- [8] V.M. Gryaznov, Sep. Purif. Meth. 29 (2000) 171–187.
- [9] A.I. Livshits, Y. Hatano, K. Watanabe, Fusion Sci. Technol. 41 (2002) 882–886.
- [10] G.M. McCracken, D.J.H. Goodall, R.T.P. Whipple, G. Long, Nucl. Fusion (Spec. Suppl.) (1974) 439–448.
- [11] R.E. Buxbaum, Sep. Sci. Technol. 18 (1983) 1251–1273.
- [12] C. Hsu, R.E. Buxbaum, J. Nucl. Mater. 141–143 (1986) 238–243.
- [13] T. Takeda, A. Ying, M.A. Abdou, Fusion Eng. Des. 28 (1995) 278–285.
- [14] A.P. Fraas, Comparative Study of the More Promising Combinations of Blanket Materials, Power Conversion Systems, and Tritium Recovery and Containment Systems for Fusion Reactors, Oak Ridge National Laboratory, Oak Ridge, 1975, pp. 1–114.
- [15] Y. Kawamura, M. Enoeda, T. Yamanishi, M. Nishi, Fusion Eng. Des. 81 (2006) 809–814.
- [16] M. Amano, M. Komaki, C. Nishimura, J. Less-Common Met. 172–174 (1991) 727–731.
- [17] K. Hashi, K. Ishikawa, T. Matsuda, K. Aoki, J. Alloys Compd. 404 (2005) 273–278.
- [18] R.E. Buxbaum, T.L. Marker, J. Membr. Sci. 85 (1993) 29–38.
- [19] S.N. Paglieri, J.R. Wermer, R.E. Buxbaum, M.V. Ciocco, B.H. Howard, B.D. Morreale, Energy Mater., in press.
- [20] S. Hayashi, J. Alloys Compd. 359 (2003) 281–286.
- [21] Y. Zhang, R. Maeda, M. Komaki, C. Nishimura, J. Membr. Sci. 269 (2006) 60–65.
- [22] J.E. Kleiner, E.H. Sevilla, R.M. Cotts, Phys. Rev. B 33 (1986) 6662–6666.
- [23] R.E. Buxbaum, R. Subramanian, J.H. Park, D.L. Smith, J. Nucl. Mater. 233–237 (1996) 510–512.
- [24] R.H. Wiswall, J.J. Reilly, Inorg. Chem. 11 (1972) 1691.
- [25] F. Botter, J. Less-Common Met. 49 (1976) 111–122.
- [26] S. Fukada, T. Yamasaki, H. Matsuo, N. Mitsubishi, J. Nucl. Sci. Technol. 27 (1990) 642–650.
- [27] C. Laquerbe, S. Contreras, O. Baudouin, J. Demoment, Fusion Sci. Technol. 54 (2008) 403–406.
- [28] R.C.J. Bowman, F.E. Lynch, R.W. Marmaro, C.H. Luo, B. Fultz, J.S. Cantrell, D. Chandra, Z. Phys. Chem., N.F. 181 (1993) 262–269.
- [29] J.J. Reilly, G.D. Sandrock, Sci. Am. 242 (1980) 118–129.
- [30] D. Chandra, J.J. Reilly, R. Chellappa, JOM 58 (2006) 26–32.
- [31] C.-H. Fagerstroem, F.D. Manchester, J.M. Pitre, in: F.D. Manchester (Ed.), Phase Diagrams of Binary Hydrogen Alloys, ASM International, Materials Park, OH, USA, 2000, pp. 273–292.
- [32] J.J. Reilly, R.H.J. Wiswall, Inorg. Chem. 9 (1970) 1678–1682.
- [33] K. Fujita, Y.C. Huang, M. Tada, J. Jpn. Inst. Met. 43 (1979) 601–610.
- [34] R. Griffiths, J. Pryde, A. Righini Brand, J. Chem. Soc., Faraday Trans. I 68 (1972) 2344–2349.
- [35] T. Schober, Solid State Phenom. 49–50 (1996) 357–422.
- [36] T. Flanagan, H. Noh, J.D. Clewley, R.C. Bowman Jr., Scripta Metall. Mater. 28 (1993) 355–359.
- [37] J.J. Reilly, R.H. Wiswall Jr., Ber. Bunsen. Phys. Chem. 76 (1972) 756.
- [38] A.J. Maeland, G.G. Libowitz, J.F. Lynch, G. Rak, J. Less-Common Met. 104 (1984) 133–139.
- [39] J.F. Lynch, G.G. Libowitz, A.J. Maeland, J. Less-Common Met. 103 (1984) 117–122.
- [40] G.G. Libowitz, A.J. Maeland, Mater. Sci. Forum 31 (1988) 177–196.
- [41] J.F. Lynch, F. Millot, J.J. Reilly, J. Phys. Chem. Solids 39 (1978) 883–890.
- [42] A. Kagawa, E. Ono, T. Kusakabe, Y. Sakamoto, J. Less-Common Met. 172–174 (1991) 64–70.
- [43] H. Yukawa, A. Teshima, D. Yamashita, S. Ito, S. Yamaguchi, M. Morinaga, J. Alloys Compd. 337 (2002) 264–268.
- [44] H. Yukawa, M. Takagi, A. Teshima, M. Morinaga, J. Alloys Compd. 330–332 (2002) 105–109.
- [45] S.W. Lambert, D. Chandra, W.N. Cathey, F.E. Lynch, R.C.J. Bowman, J. Alloys Compd. 187 (1992) 113–135.
- [46] D. Chandra, W.N. Cathey, D. Clare, H. Mandalia, W. Chien, J.R. Wermer, J.S. Holder, W.C. Mosley, in: R.G. Bautista, B. Mishra (Eds.), Rare Earths and

- Actinides: Science, Technology and Applications IV, TMS Annual Mtg., TMS, Nashville, TN, USA, 1990, pp. 73–85.
- [47] S. Bagchi, D. Chandra, W.N. Cathey, R.C. Bowman, R.B. Schwarz, F.E. Lynch, in: R.G. Bautista, C.O. Bounds, T.W. Ellis, B.T. Kilbourn (Eds.), *Rare Earths: Science, Technology & Applications III*, TMS Annual Mtg., TMS, Orlando, FL, USA, 1997, pp. 75–85.
- [48] D. Chandra, S. Bagchi, S. Lambert, W. Cathey, F. Lynch, R. Bowman Jr., *J. Alloys Compd.* 199 (1993) 93–100.
- [49] A. Sharma, *Effect of Thermal Cycling and Cold-Work on $V_{0.995}Co_{0.005}$ Hydrides*, University of Nevada, Reno, Reno, NV, USA, 1992.
- [50] D. Chandra, A. Sharma, R. Chellappa, W.N. Cathey, F.E. Lynch, R.C. Bowman, J.R. Wermer, S.N. Paglieri, *J. Alloys Compd.* 452 (2008) 312–324.
- [51] F. Lynch, Personal Communication, HCl Incorporated, Littleton, Colorado, 1990.
- [52] T. Schober, W. Pesch, *Hydrogen Energy Systems*, Pergamon, New York, 1979.
- [53] W.F. Luo, J.D. Clewley, T.B. Flanagan, *J. Chem. Phys.* 93 (1990) 6710–6722.
- [54] K. Papathanassopoulos, H. Wenzl, *J. Phys. F: Met. Phys.* 12 (1982) 1369–1381.
- [55] T.B. Massalski, H. Okamoto, P.R. Subramanian, L. Kacprzak, *Binary Alloy Phase Diagrams*, second ed., ASM International, OH, USA, 1990.
- [56] Y. Hatano, A. Livshits, Y. Nakamura, A. Busnyuk, V. Alimov, C. Hiromi, N. Ohyabu, K. Watanabe, *Fusion Eng. Des.* 81 (2006) 771–776.